FUSION OF OPTICAL AND SAR DATA FOR ESTIMATING WETLAND VEGETATION LAI

Jingjuan Liao[1], Tao Xu[1, 2], Guozhuang Shen[1]
1 Key Laboratory of Digital Earth Science, Institute of Remote Sensing and Digital Earth, Chinese Academy of Sciences, Beijing 100094, China; Email:liaojj@radi.ac.cn
2 University of Chinese Academy of Science, Beijing 100049, China

KEY WORDS: Integrated vegetation index, LAI, optical remote sensing data, SAR data

ABSTRACT: Leaf area index (LAI) is an important indicator of vegetation ecosystem health. Poyang Lake wetland is the international important wetland and its vegetation LAI is the indicator of wetland ecosystem health. In Poyang Lake wetland, vegetation grows densely, and LAI has large dynamic range. Saturation often is appeared for LAI estimation using optical remote sensing data. With the development of SAR technique, SAR remote sensing data sources are continuously enriched for supporting the various applications. Considering the complex scatting mechanisms of SAR data, we defined a radar vegetation index, and proposed a new integrated vegetation index based on the fusion of optical and SAR data. The integrated vegetation index was used for estimation of wetland vegetation LAI. The validation of measured data and theoretical model simulation showed that this integrated vegetation index is a good alternative to which using only the optical or SAR data. The best fitting models were generated using optical vegetation indices, radar vegetation index, and the integrated vegetation index, respectively. The results indicated that the integrated vegetation index can improve predication accuracy for wetland vegetation LAI.

1. INTRODUCTION

Leaf area index (LAI) is one of canopy structure parameters of vegetation. LAI of wetland vegetation is an important indicator to measure the primary productivity and ecosystem health of wetland, and control the biological and physical processes of wetland vegetation (Bonan, 1995). Traditional ground measurement can obtain LAI values from specific surface, but it is difficult to monitor a wide range of LAI. Remote sensing technology, which has the advantages of large coverage area and high efficiency, provides an effective way for LAI monitoring in regional and global vegetation (Meng et al., 2007). At present, optical remote sensing is main method of LAI remote sensing retrieval, and LAI is estimated by establishing the empirical relationship between LAI and vegetation index (VI), and VI is calculated by surface reflectance from remote sensing measurement (Liu et al., 2013). The results show that the LAI is higher, and the VI from the optical data is not sensitive to LAI, so the LAI is not able to be accurately estimated (Haboudance et al., 2004; Tang et al., 2007; Zhao et al., 2013). Synthetic Aperture Radar (SAR), which has the advantages of all-weather, day and night imaging capabilities, and its ability to penetrate the dense vegetation canopy, has great potential in the retrieval and monitoring of vegetation parameters (Yu et al., 2012; Gao et al., 2013; McNairm et al., 2014; Zhang et al., 2014). For LAI inversion, SAR has more interference factors than optical remote sensing. These factors include the system parameters, the vegetation structure, density and water content, and the soil moisture from the surface, so the mechanism of the interaction between electromagnetic wave and vegetation is more complex (Wang and Liao, 2010). Therefore, it is very useful to retrieve vegetation LAI with the combination of optical and SAR remote sensing. Some studies have focused on LAI estimation of forest and crop vegetation by integrating the optical and SAR remote sensing, but the LAI retrieval of wetland vegetation is less studied (Clevers and VanLeeuwen, 1996; Manninen et al., 2005; Gao et

al., 2013).

In the study, considering the characteristics of dense vegetation coverage and large dynamic range of LAI in Poyang Lake wetland, a new method by integrating the optical and SAR data for LAI estimation of wetland vegetation is proposed using GF-1 optical data and Radarsat-2 polarimetric data.

2. TEST SITE AND DATA

2.1 Test Site

The study site is located in the Poyang Lake Wetland in Jiangxi Province, China. Poyang Lake is an internationally important wetland and the largest freshwater lake in China. The climate is characterized as a subtropical, humid monsoon climate with a mean annual precipitation of 1620 mm and an average annual temperature of about 17 ℃. The hydrological environment of the Poyang Lake Wetland is very suitable for wetland vegetation. In the dry season (November–April), wetland vegetation emerges above water and starts to grow rapidly from early spring, with the aboveground biomass reaching the highest level in April. In the wet season (June –September), wetland vegetation is flooded and hardly grows except at the lakesides with higher ground level. In November, the water recedes and vegetation growth recommences (Liao et al., 2013). The test area in this study is located in central and western regions of Poyang Lake, as shown in Figure 1(a). Figure 1(a) is the 4-3-2 band false color composite image of GF-1 PMS1 data. In figure 1(a), blue line area shows the Radarsat-2 imaging area, the red area is the wetland vegetation of Poyang Lake. The predominant vegetation in the Poyang Lake is *Carex cinerascens Kükenth* , which accounts for over 90% of the vegetation coverage, and its real structure is shown in Figure 1(b).

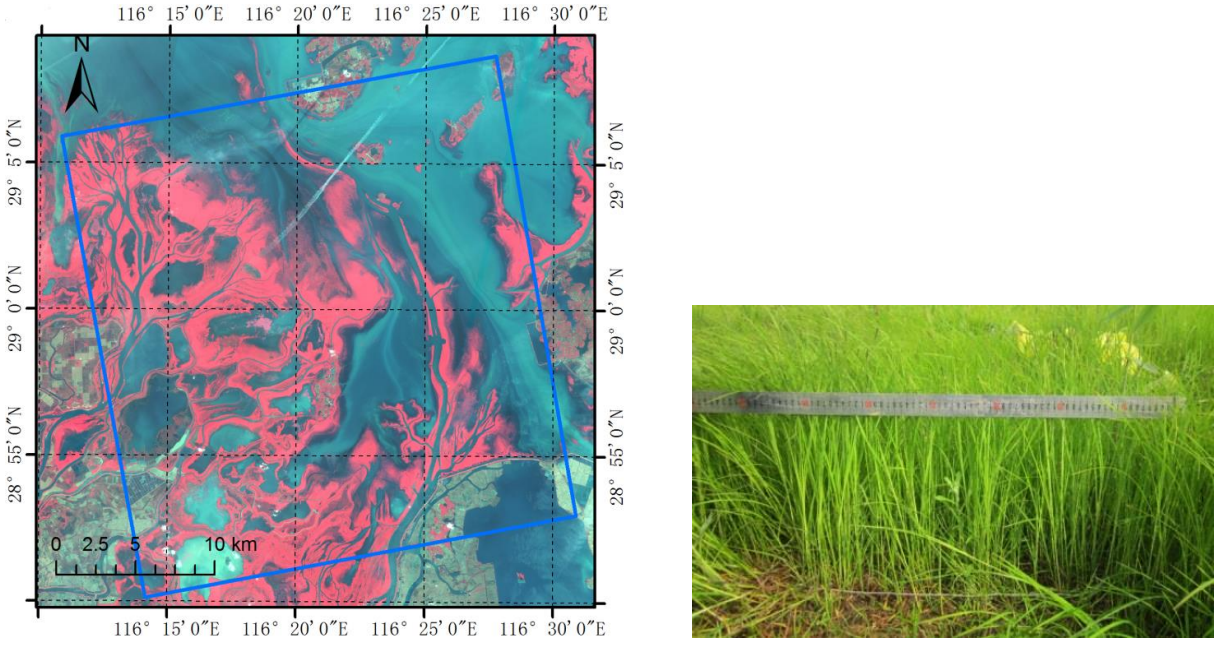

(a) (b)

Figure 1 (a) Location of Poyang Lake wetland test site; (b) Real structure of *Carex* in Poyang Lake wetland

2.2 Remote Sensing Data

In the study, we used the Level 1A product of multispectral image acquired by GF-1 PMS1 sensor on 10 April 2015, with a resolution of 8m. SAR data is SLC product acquired by the Canadian satellite Radarsat-2 with fine quad-polarization mode on 4 April 2015. The data, for which the range and azimuth pixel spacings are 4.73m and 4.96 m, with an incidence angle of 38 °.

The data processing of GF-1 includes radiation, atmospheric and geometric corrections. The GF-1 image is classified as vegetation, water and exposed-shoal for masking the LAI inversion. The SAR data processing includes

radiation calibration, Lee filter, geometric correction and extraction of the radar backscatter coefficient, and the Freeman-Durden decomposition is performed to extract three kinds of scattering components (double-bounce, volume and surface scatterings) using the Polsarpro software.

2.3 Field Measurements

Field measurements concurrent with the remote sensing data acquisition were collected from April3–9, 2015. During the field survey, 45 sampling points were collected from 0.5 × 0.5 m quadrants, and each group is averaged by 3 random sampling points. The leaf and stem characteristics, soil parameters, weight of grass, and location of the sampling point (obtained from GPS records) were recorded. The collected grasses were placed in an oven and dried for 12 hours at a constant temperature (100 ℃), following which the grass moisture was obtained. LAI was measured using LAI-2200 canopy analyzer.

3. METHODS

In the study, we established the correlation between the LAI of Poyang Lake wetland vegetation and the Radarsat-2 polarimetric and GF-1 data. The correlation is used to select the optimal parameters from optical and SAR data for LAI estimation.

3.1 Optical Vegetation Index

The Vegetation index composed by red and infrared bands is usually used for LAI estimation due to LAI is sensitive to the reflection from the two bands. In the study, three kinds of vegetation indices (Table 1), such as ratio vegetation index (RVI), normalized difference vegetation index (NDVI) and enhanced vegetation index (EVI) are used to analyze the correlation with the measured LAI in Poyang Lake wetland.

Table 1 Definitions of vegetation indices

Vegetation index	Equation
NDVI	$NDVI = (R_{Nir} - R_{\mathrm{Red}}) / (R_{Nir} + R_{\mathrm{Red}})$
RVI	$RVI = R_{Nir} / R_{\mathrm{Red}}$
EVI	$EVI = 2.5*(R_{Nir} - R_{\mathrm{Red}}) / (1 + R_{Nir} + 6*R_{\mathrm{Red}} - 7.5*R_{\mathrm{Red}})$

3.2 Radar Vegetation Index Based on the Freeman-Durden Decomposition

Radar scattering is divided into volume, double-bounce and surface scattering based on the Freeman-Durden decomposition. The total covariance matrix can be expressed as the sum of the covariance matrix of the three scattering components(Freeman and Durden, 1998):

$$C_3 = P_V C_{volume} + P_D C_{double} + P_S C_{surface} \quad (1)$$

here C_{volume}, C_{double}, $C_{surface}$ are the covariance matrix of volume, double-bounce and surface scattering, respectively, and P_V, P_D, P_S are the components of volume, double-bounce and surface scattering, respectively. The radar vegetation index based on the Freeman-Durden decomposition is:

$$RVI_{Freeman} = \frac{P_V}{P_S + P_D + P_V} \quad (2)$$

3.3 Integrated Vegetation Index for Optical and Microwave Fusion

The optical vegetation index is sensitive to low LAI, and will reach the saturation at the high LAI. Radar has the penetration ability, and has the advantage for dense vegetation detection. So the radar backscattering is sensitive to LAI, and the saturation appears in higher LAI. The vegetation index for optical and microwave fusion is proposed to estimate the LAI:

$$MNDVI = RVI_{Freeman} * (R_{Nir} - R_{Red}) / (R_{Nir} + R_{Red}) \quad (3)$$

$$MRVI = RVI_{Freeman} * R_{Nir} / R_{Red} \quad (4)$$

$$MEVI = RVI_{Freeman} * 2.5 * (R_{Nir} - R_{Red}) / (1 + R_{Nir} + 6 * R_{Red} - 7.5 * R_{Red}) \quad (5)$$

3.4 Integrated Vegetation Index Simulation Based on the Model

In order to verify the feasibility of the integrated vegetation index, the models were used to simulate the vegetation index, and the correlation between LAI and vegetation index was analyzed. PROSAIL model (Li et al., 2009) was used to simulate the optical vegetation index, and the microwave canopy scattering model proposed by Karam (1982) was used to simulate the radar backscattering for vegetation of Poyang Lake wetland. The microwave canopy scattering model was modified to simulate the radar backscattering for vegetation of Poyang Lake wetland, and the good results were obtained (Shen et al., 2015). The total backscattering of wetland vegetation includes in the volume scatterings of stem and leaf, the double-bounce introduced by the interaction between the leaf, stem, and the ground, , and the direct backscatter, and expressed as:

$$\sigma_{ij}^{total} = \sigma_{ij}^{leaf} + \sigma_{ij}^{leaf\_ground} + \sigma_{ij}^{stem} + \sigma_{ij}^{stem\_ground} + \sigma_{ij}^{ground} \quad (6)$$

here i, j are H or V. σ_{ij}^{leaf} and σ_{ij}^{stem} are the volume scatterings from leaf and stem. $\sigma_{ij}^{leaf\_ground}$ and $\sigma_{ij}^{stem\_ground}$ are the double-bounce scattering introduced by the interaction between the leaf, stem, and the ground. σ_{ij}^{ground} is the direct scattering from ground.

In the model, the leaf was modeled as a dielectric elliptical blade, and the stem was simulated with infinite length dielectric cylinder model. The integral equation model was used for surface simulation. The Debye–Cole model was used to calculate the dielectric constant of the vegetation canopy. The details of the model are referred in references (Karam and Fung, 1982; Shen et al., 2015).

For the Freeman-Durden decomposition, the total scattering power is expressed as Span:

$$Span = |S_{HH}|^2 + 2|S_{HV}|^2 + |S_{VV}|^2 = P_S + P_D + P_V \quad (7)$$

and

$$P_V = 8|S_{HV}|^2 \quad (8)$$

combined with formula (2), the radar vegetation index can be expressed as:

$$RVI_{Freeman} = \frac{8|S_{HV}|^2}{|S_{HH}|^2 + 2|S_{HV}|^2 + |S_{VV}|^2} \quad (9)$$

and the radar backscatter coefficient can be defined as follow:

$$\sigma_{ij} = \frac{4\pi}{A_0} |S_{ij}|^2 \tag{10}$$

here A_0 is he radar radiation area, so the radar vegetation index can be expressed as follow:

$$RVI_{Freeman} = \frac{8\sigma_{HV}}{\sigma_{HH} + 2\sigma_{HV} + \sigma_{VV}} \tag{11}$$

It can be simulated with the microwave canopy scattering model.

4. RESULTS AND DISCUSSION

4.1 Correlation Between the Optical Vegetation Index and LAI

The correlation between the measured LAI and the vegetation index calculated from GF-1 data is showed in Figure 2(a), and the figure shows the three vegetation indices have a certain saturation trend with the increase of LAI, which was due to the peak growth season of Poyang Lake wetland vegetation. For lower LAI, the vegetation index becomes large with the increase of LAI. The correlations between the three kinds of vegetation indices and LAI are high, and the correlation coefficient can reach 0.91. When the LAI is more than 3, the vegetation index shows a certain saturation trend, and the correlation is poor. For the vegetation of Poyang Lake wetland , the dynamic range of LAI is (0, 6). The vegetation index and LAI do not show a good correlation trend due to the phenomenon of saturation (see Figure 2(b)). So it is difficult to accurately estimate the LAI only using the GF-1 data.

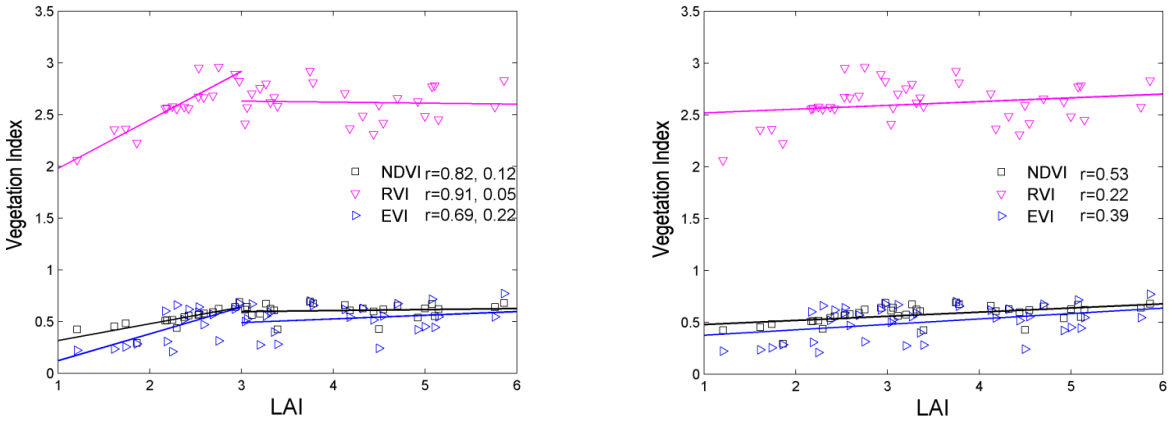

(a) (b)

Figure 2 Relationship between the optical vegetation index and LAI

4.2 Correlation Between Radarsat-2 Data and LAI

The correlation between the measured LAI and the backscattering coefficients of HH, HV, and VV polarization of Radarsat-2 data is showed in Figure 3. There is no strong correlation between the three backscattering coefficients and LAI due to the complex mechanism of radar to vegetation and the effect of the surface condition. The correlation between the backscattering coefficient of HV polarization and LAI is higher than that of HH and VV polarizations. This reason is that the HV polarization is correlated with the volume scattering, and the HH and VV polarizations reflect the double-bounce and surface scatterings.

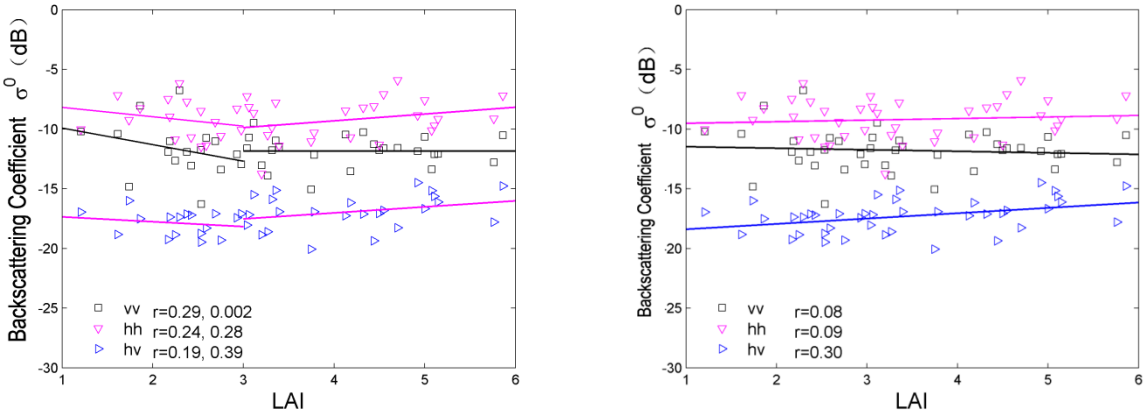

(a) (b)

Figure 3 Relationship between the backscattering coefficient and LAI

Based on the Freeman-Durden decomposition for Radarsat-2 data, the correlation between the three scattering components and LAI is analyzed (see Figure 4). The correlation between the volume scattering component and LAI is the highest, and reaches 0.54. At lower LAI value, the double-bounce component is dominant in the three scattering components. In Poyang Lake wetland, when the vegetation is sparse, the double-bounce scattering is dominant because the water content of ground surface is high and the surface is flat. Figure 5 shows the correlation between the radar vegetation index and LAI, and the correlation coefficient can reach 0.65, and it is more than the correlation between the volume scattering component and LAI. From Figure 4 and 5, when LAI is higher, the volume scattering component is dominant in the total scattering power, and double-bounce and surface scattering are poor. At low LAI value, the radar scattering is complex, and the dominant double-bounce leads to the decrease of the sensitivity of the volume scattering component to LAI.

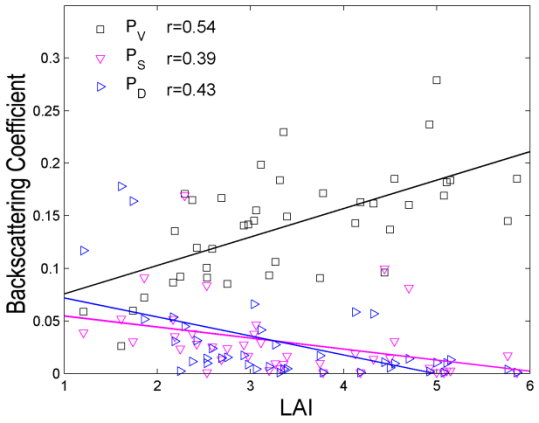

Figure 4 Relationship between the Freeman-Durden decomposition components of Radarsat-2 data and LAI

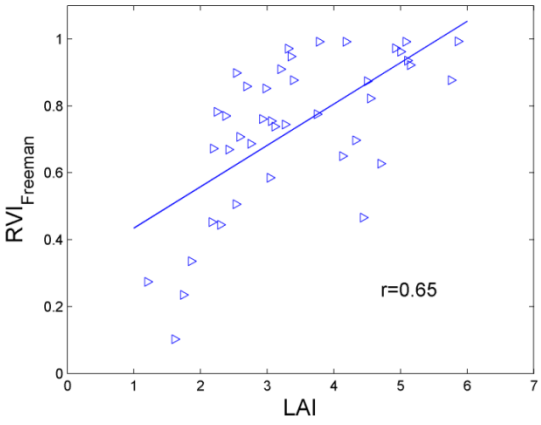

Figure 5 Relationship between the radar vegetation index and LAI

4.3 Correlation Between the Integrated Vegetation Index and LAI

Figure 6 shows the correlation between the integrated vegetation index and LAI, and the correlation is higher than that of the optical and radar vegetation indices and LAI. The highest correlation between MNDVI and LAI is 0.71.

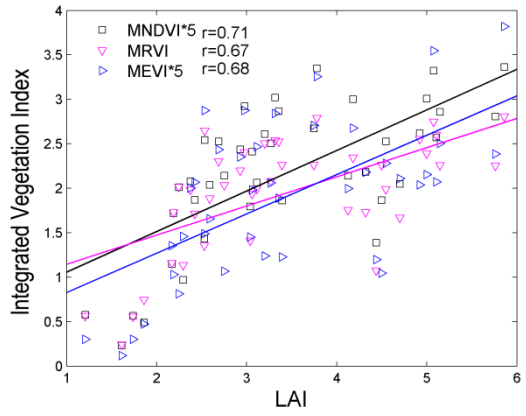

Figure 6 Relationship between the integrated vegetation indices and LAI

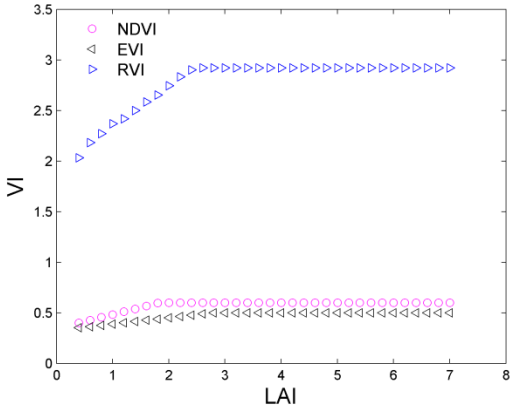

Figure 7 Relationship between the vegetation index simulated by PROSAL model and LAI

4.4 Simulation and Analysis of the Integrated Vegetation Index Based on the Model

PROSAL model was used to simulate the optical vegetation index, and the correlation between the optical vegetation index and LAI was analyzed as shown in Figure 7. The saturation points of LAI corresponding to the three kinds of vegetation indices are from 2 to 3, and increases with the increase of LAI at low LAI value.

Microwave canopy scattering model was used to simulate the radar vegetation index, and the correlation between the radar vegetation index and LAI was analyzed as shown in Figure 8. Combined with the results of the optical and radar vegetation indices, the relationship between the integrated vegetation index and LAI can be shown in Figure 9. There is very strong positive correlation between the integrated vegetation index and LAI. The integrated vegetation index can overcome the saturation from the optical vegetation index at high LAI value, and the radar vegetation index is not sensitive to LAI at low LAI value. So the integrated vegetation index can be used for LAI estimation in Poyang Lake wetland.

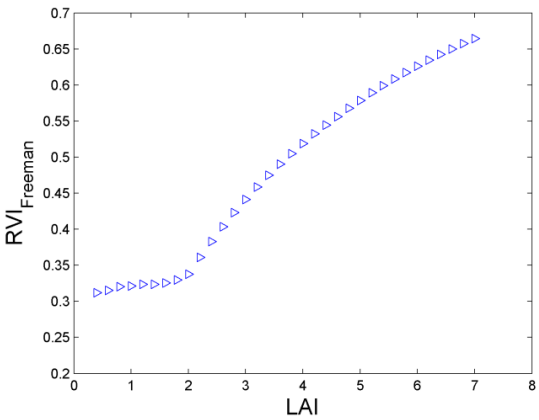

Figure 8 Relationship between the radar vegetation index simulated by microwave canopy scattering model and LAI

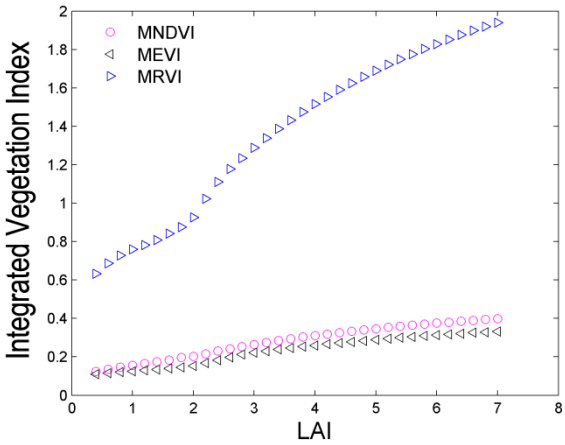

Figure 9 Relationship between the integrated vegetation indices simulated with the model and LAI

4.5 Analysis of LAI Estimation

The estimation models between the different vegetation indices and LAI are shown in Table 2, and the estimation results was analyzed using GF-1, Radarsat-2 and measured LAI data. Compared with the estimation results of the optical vegetation index, the LAI estimated by the integrated vegetation index is significant , and R^2 is more than

0.65. Compared with the radar vegetation index, the coefficients (R^2) of the three kinds of integrated vegetation indices are improved, and RSME of MNDVI is smaller, indicated that the integrated vegetation index has the advantage of combined with the optical and radar data, and improves the saturation of the optical vegetation index, and increase the sensitivity of the radar vegetation index at low LAI value, so it is more suitable for LAI estimation in Poyang Lake wetland. Considering R^2 and RSME, the model of LAI estimation from the integrated vegetation index (MNDVI) is the best, so it was used for LAI estimation in the study area.

Table 2 The estimation models between different vegetation indices and LAI

Vegetation index	Estimation model	R^2	RMSE
MNDVI	$y = 6.98 * x^{1.298}$	0.711	0.889
MRVI	$y = 1.121x + 1.247$	0.651	0.964
MEVI	$y = -2.978x^2 + 6.419x + 1.498$	0.682	0.967
NDVI	$y = 5.98 * x^{1.4}$	0.289	1.022
RVI	$y = 1.328x - 0.045$	0.124	1.183
EVI	$y = 2.933x + 1.947$	0.231	1.116
$RVI_{Freeman}$	$y = 1.43 * e^{1.146x}$	0.635	0.914

5 CONCULSIONS

In the study, based on the correlation between the LAI and vegetation index, we proposed the integrated vegetation index, which makes full use of the high sensitivity of the optical data at low LAI value and radar penetration for dense vegetation canopy. The integrated vegetation index was constructed by the optical vegetation multiplying the radar vegetation index, and the better correlation between the integrated vegetation index and LAI was verified by the analysis of the measured data and the model simulation. For the three kinds of integrated vegetation indices, the coefficients (R^2) of the estimation model are more than 0.65, and the estimation model from MNDVI is the best.

The method of LAI estimation using the integrated vegetation is simple and easy to use. In future work, the integrated vegetation index will be improved to estimate the LAI of different type vegetation.

References

[1] Bonan G B. Land atmosphere Interactions for Climate System Models: Coupling Biophysical, Biogeochemical and Ecosystem Dynamical Processes[J]. Remote Sensing of Environment, 1995, 51(1): 57-73.

[2] Clevers, JGPW, VanLeeuwen HJC. Combined use of optical and microwave remote sensing data for crop growth monitoring[J]. Remote Sensing of Environment, 1996, 56(1): 42-51.

[3] Freeman A, Durden S L. A Three-component Scattering Model for Polarimetric SAR Data[J]. IEEE Trans. Geosci. Remote Sens. 1998, 36(3), 963-973.

[4] Gao S, Niu Z, Huang N, et al. Estimating the Leaf Area Index, height and biomass of maize using HJ-1 and RADARSAT-2[J]. International Journal of Applied Earth Observation and Geoinformation, 2013, 24: 1-8.

[5] Gao Shuai, Niu Zheng, Wu Mingquan. The neural network algorithm for estimation plantation forest leaf area index based on ENVISAT/ASAR[J]. Remote Sensing Technology and Application, 2013, 28(2): 205-211.

[6] Haboudane D, Miller J R, Pattey E, et al. Hyper-spectral vegetation indices and novel algorithms for predicting green LAI of crop canopies: modeling and validation in the context of precision agriculture[J]. Remote Sensing of Environment, 2004, 90(3): p. 337-352.

[7] Karam M A, Fung A K. Propagation and Scattering in Multi-layered Random Media with Rough Interface[J]. Electromagnetics, 1982, 2: 239-256.

[8] Li Shumin, Li Hong, Sun Danfeng, et al. Estimation of regional leaf area index by remote sensing inversion of PROSAIL canopy spectral model[J]. Spectroscopy and Spectral Analysis 2009, 29(10): 2725-2729.

[9] Liao Jingjuan, Shen Guozhuang，Dong Lei, Biomass estimation of wetland vegetation in Poyang Lake area using ENVISAT advanced synthetic aperture radar data, Journal of Applied Remote Sensing, 2013, Vol.7, 073579

[10] Liu Yang, Liu Ronggao, Chen Jingming, et al. Current status and perspectives of leaf area index retrieval from optical remote sensing data[J]. Journal of GEO-Information Science, 2013, 15(5): 734-743.

[11] Manninen T, Smolander H, Voipio P, et al. Boreal forest LAI retrieval using both optical and microwave data of ENVISAT[C]. Geoscience and Remote Sensing Symposium. IGARSS'95, 2005, 7: 5033-5036.

[12] McNairm H, Kross A, Lapen D, et al. Early season monitoring of corn and soybeans with TerraSAR-X and RADARSAT-2[J]. International Journal of Applied Earth Observation and Geoinformation, 2014, 28: 252-259.

[13] Meng Jihua, Wu Bingfang, Li Qiangzi. Method for estimating crop leaf area index of China using remote sensing[J]. Transaction of the CSAE, 2007, 23(2): 160-167.

[14] Shen G Z, Liao J J, Guo H D, et al. Journal of Applied Remote Sensing. Poyang Lake wetland vegetation biomass inversion using polarimetric RADARSAT-2 synthetic aperture radar data[J]. 2015, 9, 096077.

[15] Tang S, Chen J M, Zhu, Q, et al. LAI inversion algorithm based on directional reflectance kernels[J]. Journal of Environmental Management, 2007, 85(3): 638-648.

[16] Wang Qing, Liao Jingjuan. Estimation of wetland vegetation biomass in the Poyang Lake area using Landsat TM and ENVISAT ASAR data[J]. Journal of GEO-Information Science, 2010, 12(2): 2282-2291.

[17] Yu Fan, Zhao Yingshi, Li Haitao. Soil moisture retrieval based on GA-BP neural networks algorithm[J]. Journal of Infrared and Millimeter Waves, 2012, 31(3): 283-288.

[18] Zhang Y, Liu X H, Su S L. Retrieving canopy height and density of paddy rice from Radarsat-2 images with a canopy scattering model[J]. International Journal of Applied Earth Observation and Geoinformation, 2014, 28: 170-180.

[19] Zhao Juan, Huang Wenjiang, Zhang Yaohong, et al. Inversion of leaf area index during different growth stages in winter wheat[J]. Spectroscopy and Spectral Analysis, 2013, 33(9): 2546-2552.